RSC Advances

ROYAL SOCIETY OF CHEMISTRY

www.rsc.org/advances

The structural and magnetic properties of Tm$_5$Ge$_4$ compound

Junding Zou,[*ab] Mi Yan[*a], and Jinlei Yao[c]

[a] *School of Materials Science and Engineering, State Key Laboratory of Silicon Materials, Key Laboratory of Novel Materials for Information Technology of Zhejiang Province, Zhejiang University, Hangzhou, Zhejiang 310027, China.* zoujd@zju.edu.cn *(J. D. Zou),* mse_yanmi@zju.edu.cn *(M. Yan). Tel: 86-571-87952366.*

[b] *Ames Laboratory, U.S. Department of Energy, and Iowa State University, Ames, Iowa 50011-3020, USA*

[c] *Research Center for Solid State Physics and Materials, School of Mathematics and Physics, Suzhou University of Science and Technology, Suzhou 215009, China*

So far, Tm$_5$Ge$_4$ compound is the last one in R$_5$Ge$_4$ (R= rare earth elements with magnetic moments) compounds family (exclusive of Pm and Eu) whose magnetic properties are still unknown. We prepare high quality Tm$_5$Ge$_4$ compound, and report the detailed crystal structure and magnetic properties. Tm$_5$Ge$_4$ crystallizes in the Sm$_5$Ge$_4$-type orthorhombic structure at room temperature, and orders antiferromagnetically at T'_N=13 and T_N=21 K, respectively. The paramagnetic Curie temperature of Tm$_5$Ge$_4$ is positive (θ_p=16 K), and the effective magnetic moment (p_{eff}=7.4 μ_B/Tm) is in good agreement with the theoretical value of 7.56 μ_B/Tm^{3+}. The ac susceptibility of Tm$_5$Ge$_4$ shows obvious frequency dependence behaviors suggesting the existence of ferromagnetic cluster in the antiferromagnetic substance. According to the magnetic hysteresis loop, the intrinsic coercivity of Tm$_5$Ge$_4$ is 2616 Oe at 2 K. Tm$_5$Ge$_4$ exhibits oscillating magnetocaloric

effect owing to a metamagnetic-like transformation induced by a critical magnetic field below 21 K.

1. Introduction

The pseudobinary $R_5(Si,Ge)_4$ (R=rare earth elements) compounds form an extraordinary large family, and have received considerable attention due to their unique magnetic properties, e.g., giant magnetocaloric effect (MCE) ,[1, 2] magnetostritive effect,[3] magnetoresistence effect,[4,5] and Griffiths-like phase behavior. [6, 7,8, 9] Depending on the different bonding types between the slabs (each slab represents half of the unit cell along the longest b-direction and is infinite in the a- and c-directions), $R_5(Si,Ge)_4$ compounds can form Gd_5Si_4-type orthorhombic structure (space group: Pnma), $Gd_5Si_2Ge_2$-type monoclinic structure (space group: $P112_1/a$), Sm_5Ge_4-type orthorhombic structure (space group: Pnma) and $Tm_5Si_2Sb_2$-type orthorhombic structure (space group: Ccmb). [10, 11] Usually, the magnetic moments of rare earth atoms that belong to the same slab are aligned ferromagnetically (FM) in the c-direction. The direction of the moments may be reversed from one slab to another in the antiferromagnetic (AFM) structure, while the directions of the moments are the same in all slabs in the FM structure. Furthermore, the crystallography and magnetism in $R_5(Si,Ge)_4$ compounds are found to be closely related. The FM orderings usually appear when all slabs are interconnected (Gd_5Si_4-type structure), while AFM orderings can be observed in some compounds with Sm_5Ge_4-type orthorhombic structure in which none slab is interconnected. The paramagnetic (PM) states can exist when none (Sm_5Ge_4-type structure), one-half ($Gd_5Si_2Ge_2$-type structure), or all (Gd_5Si_4-type structure) slabs are interconnected.[10, 11] For many $R_5(Si,Ge)_4$ compounds, magnetic phase transitions coupled with crystal structure transformation are

observed, and can be controlled by magnetic field, temperature, pressure, as well as elemental substitution.[1,2, 3, 12, 13,14]

Among pseudobinary $R_5Si_xGe_{4-x}$ compounds, the parent compounds R_5Ge_4 usually show very complex magnetic phase diagrams and interesting magnetic behaviors. So far, no proof indicates that Pm and Eu can combine with Ge to form 5:4-type compounds. Although the crystal structure of Tm_5Ge_4 compound have been reported in past, [15, 16] it is still the last one in R_5Ge_4 compounds family whose magnetic properties are unknown. R_5Ge_4 compounds often show some common features. Most of R_5Ge_4 (R=rare earth elements with net magnetic moments) compounds crystallize in Sm_5Ge_4-type structures, and show AFM order at low temperature.[11, 15, 17, 18, 19, 20, 21, 22, 23, 24, 25, 26, 27, 28, 29, 30] It is interesting that the ground states of R_5Ge_4 may be FM, but the development of the equilibrium FM ordering were inhibited by a kinetic arrest of the first-order AFM-FM transition. [31] In addition, first-order magnetostructural phase transition from AFM ordering (Sm_5Ge_4-type orthorhombic structure) to FM ordering (Gd_5Si_4-type orthorhombic structure) can be induced by the application of either magnetic field, or hydrostatic pressure. Note that Ce_5Ge_4 and Yb_5Ge_4 are two exceptions. The Sm_5Ge_4-type Ce_5Ge_4 compound is FM ordering below 12 K, [32] and the Gd_5Si_4-type Yb_5Ge_4 compounds is AFM ordering below 3.2 K.[33]

Although the magnetic properties of Tm_5Ge_4 compound are still unknown, the magnetic properties of the single crystal $Tm_5Si_2Ge_2$ [34] have been studied. $Tm_5Si_2Ge_2$ showed AFM ordering along the *b*-axis below ~8 K with the FM coupled magnetic moments in the *a-c* plane. [34] The previous report had confirmed that Tm_5Ge_4 compound could be frabricated by arc-melting, and crystallized in Sm_5Ge_4-type orthorhombic

3

structure.[15,16] However, it is not easy to obtain high quality Tm_5Ge_4 compound by arc-melting method due to serious volatility of Tm and the perverse impurity phases of $Tm_{11}Ge_{10}$ and Tm_5Ge_3 which have very close chemical compositions. The synthesis method needs to be further studied in order to guarantee the high quality of Tm_5Ge_4 sample, and the magnetic properties of Tm_5Ge_4 need to be uncovered in order to gain a complete understanding of the magnetism of R_5Ge_4 compounds family.

In this work, we used induction furnace to prepare high quality Tm_5Ge_4 compound. The detailed crystal structure, magnetic properties, and phase transitions of Tm_5Ge_4 were investigated by x-ray powder diffraction (XRD), magnetic, and heat capacity measurements. We also measured the ac magnetic susceptibility and confirmed the existence of the magnetic cluster in Tm_5Ge_4.

2. Experimental details

Polycrystalline Tm_5Ge_4 sample was prepared by induction-melting of pure metals using a multi-step procedure. Tm metal was obtained from the Materials Preparation Center of the Ames Laboratory and its purity was exceeding 99.99 wt.% with respect to all other elements in the Periodic Table. [35] Ge element was bought from commercial vendor, and its purity was 99.9 wt.%. Excess amount of Tm (2 at.%) was added to compensate the evaporation lost during the induction-melting. The pure metals were sealed in a tantalum crucible (length 45mm, diameter 9.5mm) in helium atmosphere. The mixture was melted at 2133 K for 7 mins, cooled down to 1195 K (holding for 1 hr), further cooled down to 1123 K (holding for 2 hrs), then cooled down to 973 K (holding for 2 hrs) before finally powering off the induction furnace.

A single phase Tm_5Ge_4 sample with Sm_5Ge_4-type orthorhombic structure (space group Pnma) was confirmed by XRD study at room temperature performed on a Philips PANalytical powder diffractometer employing monochromatic Cu $K\alpha_1$ radiation. The lattice parameters were determined by performing Reitveld refinement using Rietica-LHPM. [36] The content of the minor phase Tm_5Ge_3 is ~2 wt.%. The dc and ac magnetization measurements were performed using a Quantum Design magnetic properties measurement system (MPMS) and physical properties measurement system (PPMS). Heat capacity measurement was conducted using PPMS. MCE (isothermal entropy change) was calculated from the heat capacity data by using $\Delta S(T) = \int_0^T \frac{C_H(T) - C_0(T)}{T} dT$ where S is the total entropy change, T is temperature, H is magnetic field, and C is heat capacity.

3. Results and discussion

The observed and calculated room-temperature XRD patterns of Tm_5Ge_4 are displayed in Fig.1(a). The Sm_5Ge_4-type orthorhombic structure of Tm_5Ge_4 compound is shown in Fig. 1(b). The refined structural parameters are summarized in Table I. The refined lattice parameters are a=7.4564(2) Å, b=14.3234(5) Å, c=7.5320(2) Å, and unit cell volume V= 804.4(4) $Å^3$ which are in agreement with the previous report.[16] The distance of Ge atoms between the slabs, as represented in Fig.1(b), are 4.4 and 3.5 Å, respectively, indicating no chemical bonds between the slabs.

As mentioned in introduction part, Er_5Ge_4 compound adopts Sm_5Ge_4-type structure,[30] and Yb_5Ge_4 compound crystallizes in Gd_5Si_4-type structure.[33] Nevertheless, both Er_5Ge_4 and Yb_5Ge_4 show AFM order. [30, 33] Therefore, it is interesting to study the case of Tm_5Ge_4 in order to reveal the variation tendency of magnetic behaviors between

Er$_5$Ge$_4$ and Yb$_5$Ge$_4$ compounds. The temperature dependence magnetizations of Tm$_5$Ge$_4$ measured in zero-field-cooled warming (ZFC), field-cooled cooling (FCC), and field-cooled warming (FCW) protocols are shown in Fig. 2. Unlike Er$_5$Ge$_4$ with only one AFM ordering,[30] Tm$_5$Ge$_4$ shows a peak at 21 K corresponding to AFM ordering temperature T_N and an additional peak at 13 K suggesting another possible AFM ordering temperature $T_N^{'}$ in a magnetic field of 50 Oe, as shown in Fig. 2(a). The hollow between two peaks appears at 18 K. Above the antiferromagnetic transition temperature, T_N=21 K, the ZFC, FCC, and FCW curves are identical. However, significant differences including irreversible thermomagnetic behavior are observed below T_N (see inset of Fig.2a). Insets of Fig. 2(a) and 2(b) enlarge the phase transition region ranging from 14 to 24 K and 13 to 24 K, respectively. Noticeable hysteresis between the FCC and FCW curves suggest that the transition observed near 18 K is a first-order phase transition.[37] The first-order nature of this transition was also identified in the behavior of heat capacity. The inverse magnetic susceptibility of Tm$_5$Ge$_4$ obeys the Curie-Weiss law. The obtained paramagnetic Curie temperature θ_p is +16 K, and the effective magnetic moment p_{eff} is 7.4μ_B/Tm which is in good agreement with the theoretical value of 7.56 μ_B/Tm^{3+}. The positive θ_p indicates that ferromagnetic interactions are dominant in the ground state. This result is similar to Gd$_5$Ge$_4$ which is found to order antiferromagnetically at 127 K but with a positive paramagnetic Curie temperature of 94 K due to the competing exchange interactions present in this compound.[38] Magnetic field can drive $T_N^{'}$ of Tm$_5$Ge$_4$ moving downward to lower temperature, and reaching 8 K at 1 kOe and 5 K at 10 kOe, respectively. This behavior indicates that the magnetic ordering at $T_N^{'}$ is AFM. The peak at 21 K will disappear when the magnetic field is higher than 10 kOe. Thermal

hysteresis behavior and peak cannot be observed in M-T curves any more in 50 kOe magnetic field, and Tm_5Ge_4 changes into a FM state in that condition. Now we win a whole picture of R_5Ge_4 compounds. R_5Ge_4 compounds (R= Ce, Pr, Nd, Sm, Gd, Tb, Dy, Ho, Er, Tm) crystalize in Sm_5Ge_4-type orthorhombic structure, while Yb_5Ge_4 crystallize in Gd_5Si_4-type orthorhombic structure. R_5Ge_4 compounds (R= Pr, Nd, Sm, Gd, Tb, Dy, Ho, Er, Tm, Yb) exhibit AFM orderings, while Ce_5Ge_4 shows FM ordering.

Figure 3 presents the ac magnetic susceptibility at different frequencies under zero dc magnetic field and 5 Oe ac magnetic field. The real component of ac susceptibility shows a peak at 22.4 K which is corresponding to T_N, see Fig.3(a). No peak is observed at 13 K in the real component of ac susceptibility, but a peak appears at 8.8 K at 10 Hz which coincides with T'_N observed in the temperature dependence of magnetization at 1 kOe, see Fig. 2(b). The peak at 8.8 K is almost unchanged till the frequency increases to 2997 Hz, but the magnitude reduces with the increase of frequency. The imaginary component of the ac magnetic susceptibility only shows a peak at 11 K (10 Hz) which increases and shifts upward to 12.8 K at 2997 Hz, as shown in Fig.3(b). The notable frequency dependence of ac susceptibility observed below 22.4 K suggests the existence of FM cluster embedding in the AFM substance. The spin glass usually originates from the magnetic frustration or crystal disorder, and also can show the frequency dependence of ac susceptibility.[39,40,41,42,43,44] The frequency sensitivity $K=\Delta T_f/[T_f\Delta\log(2\pi f)]$ can be used to determine the presence of spin-glass phase where T_f is spin-glass transition temperature and f is the frequency of ac susceptibility.[39,41] K of Tm_5Ge_4 at T'_N (taken as the peak in M'') is about 0.04 which is higher than the conventional spin-glass system

$(0.005–0.01).$[39] Apparently, the possibility of spin glass is excluded because there is no magnetic frustration or crystal disorder in Tm_5Ge_4 compound.

Figure 4 shows the magnetic hysteresis loop and isothermal magnetization of Tm_5Ge_4. The magnetic hysteresis loop at 2 K is symmetric, as shown in Fig.4(a). The intrinsic coercivity is 2616 Oe. Figure 4(b) shows the isothermal magnetization from 3 K to 39 K. Tm_5Ge_4 shows complex behavior in the low magnetic field region due to the AFM orderings. The magnetizations increase on heating, then decrease with further increasing temperature, and finally increase again with increasing temperature. Taking into account the behaviors shown in M-T and M-H curves, Tm_5Ge_4 compound exhibit the metamagnetic-like transformation (AFM↔FM) in a critical magnetic field around 6 kOe at 3 K. The critical magnetic field will decrease on heating.

Figure 5a show the heat capacity of Tm_5Ge_4 as a function of temperature and magnetic field. Unlike the complex magnetic properties, the heat capacity data show very simple behavior. The lambda-type anomaly, observed in zero magnetic field around 21 K, corresponds to the AFM ordering temperature T_N which is observed at the same temperature in the low magnetic field dc magnetization data. Behavior of the heat capacity in nonzero magnetic fields is consistent with the isothermal magnetization of Tm_5Ge_4, and the lambda-type peak slightly shifts downward with increasing magnetic field suggesting a metamagnetic-like transformation. The peak changes into broaden and smooth in 20 kOe magnetic field. There is no anomaly observed at $T_N{'}$ in heat capacity curve suggesting the near zero energy difference between AFM and FM states. The MCE feature also provides a useful tool to probe the phase transitions and magnetic states in complex magnetic systems.[45] Figure 5b show the total entropy change calculated from

heat capacity data. Tm_5Ge_4 shows oscillating MCE behavior, and the entropy change peaks for a magnetic field change ΔH=20 kOe appear at 7 K (-1.4 J/kg K) and 17 K (1.0 J/kg K), respectively. MCE of Tm_5Ge_4 is associated with the metamagnetic-like transformation induced by magnetic field.

4. Conclusions

Tm_5Ge_4 compound crystallizes in Sm_5Ge_4-type orthorhombic structure, and show complex AFM ordering at T_N=21 K and T'_N=13, respectively. AFM ordering will change into FM ordering in 50 kOe magnetic field. The ac susceptibility measurements confirm the AFM ordering, and show obvious frequency dependence behaviors suggesting the existence of FM cluster. Magnetic hysteresis loop shows symmetric characteristic, and the intrinsic coercivity at 2 K is as large as about 2616 Oe. According to the specific heat measurements, a small and lambda-like peak is observed at 21 K confirming the AFM ordering temperature T_N. Tm_5Ge_4 compound exhibits a metamagnetic-like transformation when the magnetic field exceeds a critical value leading to obvious oscillating MCE.

Acknowledgements

Notes and references

[1] V. K. Vitalij and K. A. Gschneidner, Jr., *Phys. Rev. Lett.* **78**, 4494 (1997).

[2] V. K. Vitalij and K. A. Gschneidner, Jr., *Appl. Phys. Lett.* **70**, 3299 (1997).

[3] L. Morellon, P. A. Algarabel, M. R. Ibarra, J. Blasco, B. Garcia-Landa, Z. Arnold, and F. Albertini, *Phys. Rev. B* **58**, R14721 (1998).

[4] L. Morellon, J. Stankiewicz, B. Garcia-Landa, P. A. Algarabel, and M. R. Ibarra, *Appl. Phys. Lett.* **73**, 3462 (1998).

[5] E. M. Levin, V. K. Pecharsky, and K. A. Gschneidner, Jr., *Phys. Rev. B* **60**, 7993 (1999).

[6] F. Casanova, S. de Brion, A. Labarta, and X. Batlle, *J. Phys. D: Appl. Phys.* **38**, 3343 (2005).

[7] C. Magen, P. A. Algarabel, L. Morellon, J. P. Araujo, C. Ritter, M. R. Ibarra, A. M. Pereira, and J. B. Sousa, *Phys. Rev. Lett.* **96**, 167201 (2006).

[8] Z. W. Ouyang, V. K. Pecharsky, K. A. Gschneidner, Jr., D. L. Schlagel, and T. A. Lograsso, *Phys. Rev. B* **74**, 094404 (2006).

[9] J. D. Zou, J. Liu, Y. Mudryk, V. K. Pecharsky, and K. A. Geschneidner, Jr., *J. Appl. Phys.* **114**, 063904 (2013).

[10] K. A. Gschneidner, Jr., V. K. Pecharsky, and A. O. Tsokol, *Rep. Prog. Phys.* **68**, 1479 (2005).

[11] V. K. Pecharsky and K. A. Gschneidner, Jr., *Pure Appl. Chem.* **79**, 1383 (2007).

[12] C. Magen, L. Morellon, P. A. Algarabel, M. R. Ibarra, Z. Arnold, J. Kamarad, T. A. Lograsso, D. L. Schlagel, V. K. Pecharsky, A. O. Tsokol, and K. A. Gschneidner, Jr., *Phys. Rev. B* **72**, 024416 (2005).

[13] L. Morellon, P. A. Algarabel, C. Magen, M. R. Ibarra, and Y. Skorokhod, *J. Phys.: Condens. Matter* **16**, 1623 (2004).

[14] A. Magnus G. Carvalho, Cleber S. Alves , Ariana de Campos , Adelino A. Coelho , Sergio Gama , Flavio C. G. Gandra , Pedro J. von Ranke , and Nilson A. Oliveira , *J. Appl. Phys.* **97**, 10M320 (2005).

[15] G. S. Smith, A. G. Tharp, and Q. Johnson, *Acta Cryst.* **22**, 940 (1967).

[16] V. N. Eremenko, K. A. Meleshevich, Y. I. Buyanov, and P. S. Martsenyuk, *Soviet Powder Metall. and Met. Ceramics* **28**, 543 (1989).

[17] G. S. Smith, Q. Johnson, and A. G. Tharp, *Acta Cryst.* **22**, 269 (1967).

[18] F. Holtzberg, R. J. Gambino, and T. R. McGuire, *J. Phys. Chem. Solids* **28**, 2283 (1967).

[19] H. F. Yang, G. H. Rao, W. G. Chu, G. Y. Liu, Z. W. Ouyang, and J. K. Liang, *J. Alloys Compd.* **339**, 189 (2002).

[20] G. H. Rao, Q. Huang, H. F. Yang, D. L. Ho, J. W. Lynn, and J. K. Liang, *Phys. Rev. B* **69**, 094430 (2004).

[21] P. Schobinger-Papamantellos and A. Niggli, *J. Phys. Chem. Solids* **42**, 583 (1981).

[22] J. M. Cadogan, D. H. Ryan, Z. Altounian , H. B. Wang , and I. P. Swainson, *J. Phys.: Condens. Matter* **14**, 7191 (2002).

[23] V. K. Pecharsky and K. A. Geschneidner, Jr., *J. Alloys Compd.* **260**, 98 (1997).

[24] P. Schobinger-Papamantellos, *J. Phys. Chem. Solids* **39**, 197 (1978).

[25] C. Ritter , L. Morellon , P. A. Algarabel , C. Magen , and M. R. Ibarra, *Phys. Rev. B* **65**, 094405 (2002).

[26] W. Tian , A. Kreyssig , J. L. Zarestky , L. Tan , S. Nandi , A. I. Goldman , T. A. Lograsso , D. L. Schlagel , K. A. Gschneidner , Jr., V. K. Pecharsky , and R. J. McQueeney, *Phys. Rev. B* **80**, 134422 (2009).

[27] V. V. Ivtchenko, V. K. Pecharsky, and K. A. Geschneidner, Jr., *Adv. Cryog. Eng.* **46**, 405 (2000).

[28] N. K. Singh, D. Paudyal , Ya Mudryk , V. K. Pecharsky , and K. A. Gschneidner, Jr., *Phys. Rev. B* **79**, 094115 (2009).

[29] C. Ritter , C. Magen , L. Morellon , P. A. Algarabel , M. R. Ibarra , A. M. Pereira , J. P. Araujo , and J. B. Sousa, *Phys. Rev. B* **80**, 104427 (2009).

[30] A. O. Pecharsky, K. A. Gschneidner, Jr., V. K. Pecharsky, D. L. Schlagel, and T. A. Lograsso, *Phys. Rev. B* **70**, 144419 (2004).

[31] S. B. Roy, M. K. Chattopadhyay, P. Chaddah, J. D. Moore, G. K. Perkins, L. F. Cohen, K. A. Gschneidner, Jr., and V. K. Pecharsky, *Phys. Rev. B* **74**, 012403 (2006).

[32] R. Nirmala, A. V. Morozkin, Jagat Lamsal, W. B. Yelon, and S. K. Malik, *J. Appl. Phys.* **107**, 09E308 (2010).

[33] Kyunghan Ahn, A. O. Tsokol, Yu. Mozharivskyj, K. A. Gschneindner, Jr., and V. K. Pecharsky, *Phys. Rev. B* **72**, 054404 (2005).

[34]   J. H. Kim, S. J. Kim, C. I. Lee, M. A. Jung, H. J. Oh, Jong-Soo Rhyee, Younghun Jo, H. Mitani, H. Miyazaki, Shin-ichi Kimura, and Y. S. Kwon, *Phys. Rev. B* **81**, 104401 (2010).

[35]   Materials Preparation Center, Ames Laboratory US-DOE, Ames, IA, USA, [www.mpc.ameslab.gov].

[36] B. Hunter, Rietica-*A Visual Rietveld Program, International Union of Crystallography Commission on Powder Diffraction Newsletter*, No. 20 (Summer, 1998), [http://www.rietica.org.]

[37]   M. Khan, Y. Mudryk, K. A. Gschneidner, Jr., and V. K. Pecharsky, Phys. Rev. B **82**, 064421 (2010).

[38]   E. M. Levin, K. A. Gschneidner, Jr., and V. K. Pecharsky, Phys. Rev. B **65**, 214427 (2002).

[39]   J. A. Mydosh, *Spin Glass*: *An Experimental Introduction* (Taylor & Francis, London, 1993).

[40]   D. N. H. Nam, K. Jonason, P. Nordblad, N. V. Khiem, and N. X. Phuc, Phys. Rev. B **59**, 4189 (1999).

[41]   M. K. Singh, W. Prellier, M. P. Singh, R. S. Katiyar, and J. F. Scott, Phys. Rev. B **77**, 144403 (2008).

[42]   F. Wang, J. H. Kim, and Y. J. Kim, Phys. Rev. B **80**, 024419 (2009).

[43]   M. H. Phan, N. A. Frey, M. Angst, J. de Groot, B. C. Sales, D. G. Mandrus, and H. Srikanth, Solid State Commun. **150**, 341 (2010).

[44]   E. Ilker and A. N. Berker, Phys. Rev. E **89**, 042139 (2014).

45 P. Lampen, N. S. Bingham, M. H. Phan, and H. Srikanth, Phys. Rev. B **89**, 144414

(2014).

Table 1. Crystallographic parameters of Tm_5Ge_4 at room temperature (RT).

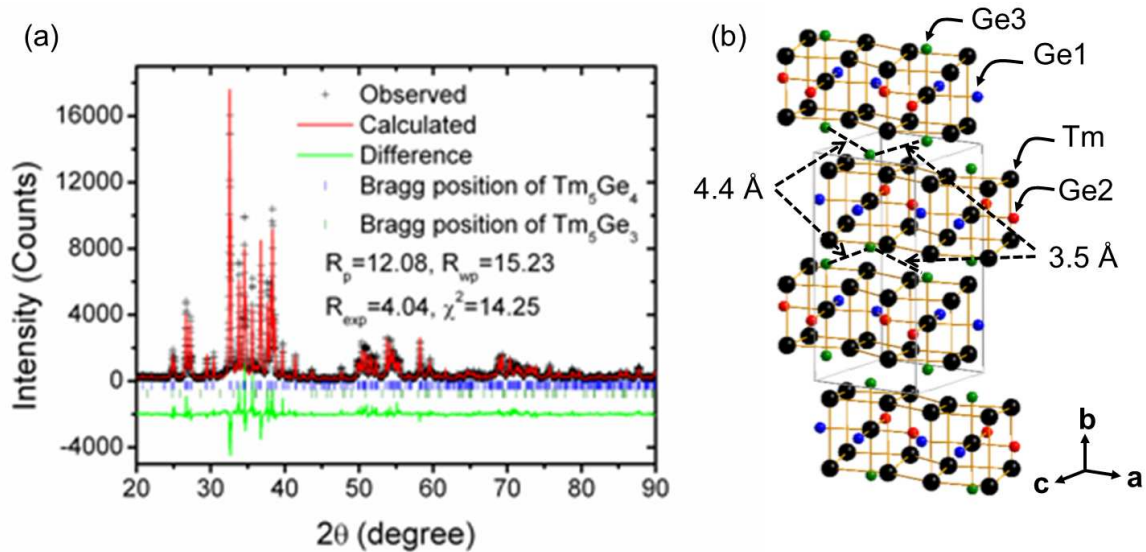|	atom	x/a	y/b	z/c	$B_{overall}$ $(Å^2)$	occupancy
Tm_5Ge_4 @RT	Tm1(4c)	0.2045(6)	1/4	-0.0001(6)	0.336(7)	0.50
	Tm2(8d)	0.0250(4)	0.0988(2)	0.6812(4)	0.336(7)	1.00
	Tm3(8d)	0.3739(4)	0.1203(2)	0.3382(4)	0.336(7)	1.00
	Ge1(4c)	0.0727(1)	1/4	0.3856(1)	0.336(7)	0.50
	Ge2(4c)	0.3354(1)	1/4	0.6418(1)	0.336(7)	0.50
	Ge3(8d)	0.2175(9)	0.0463(4)	0.0263(9)	0.336(7)	1.00
Sm_5Ge_4-type	a=7.4564(2) Å, b=14.3234(5) Å, c=7.5320(2)Å, V=804.4(4) $Å^3$					
(S.G. Pnma)	Rp=12.08, Rwp=15.23, Rexp=4.04, χ^2=14.25					

FIG.1. (Color online) (a) The observed and calculated powder XRD patterns of Tm_5Ge_4.

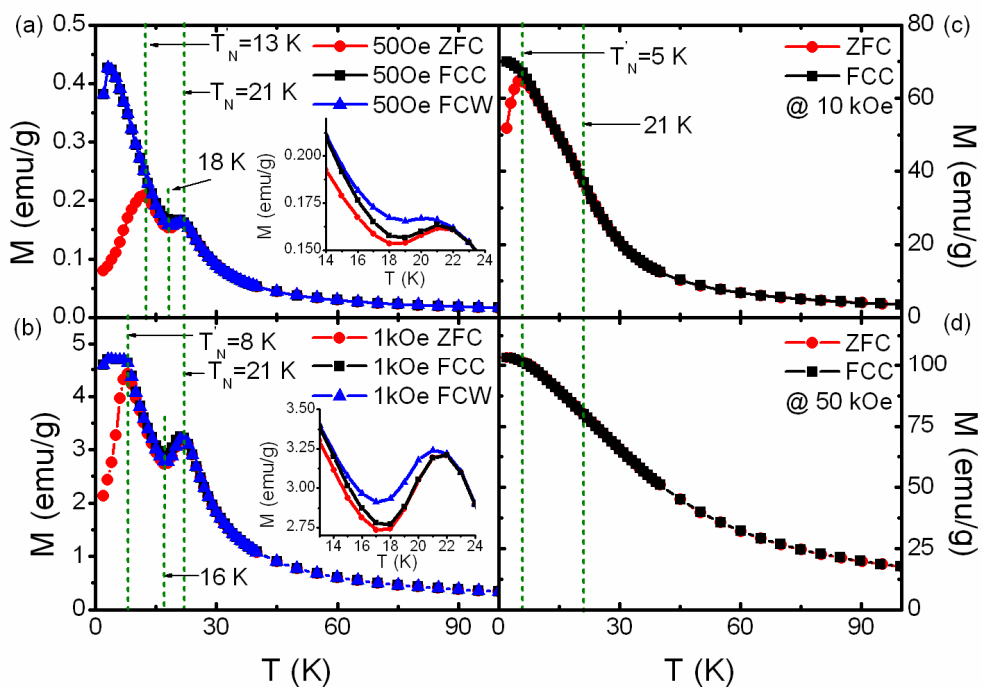(b) The Sm_5Ge_4-type orthorhombic structure of Tm_5Ge_4.

FIG.2. (Color online) The ZFC, FCC and FCW temperature dependence of the magnetizations of Tm_5Ge_4 measured in different magnetic fields. Insets of (a) and (b) enlarge the phase transition region ranging from 14 to 24 K and 13 to 24 K, respectively.
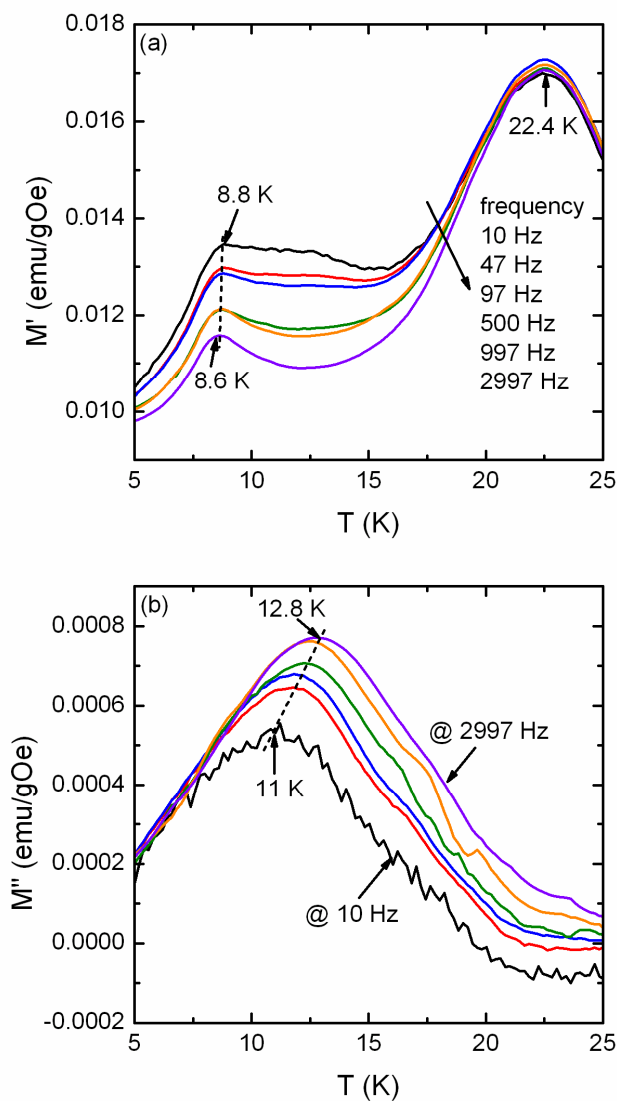
FIG.3. (Color online) (a) The real components of ac magnetic susceptibility measured as

a function of temperature and frequency on heating. (b) The imaginary components of ac
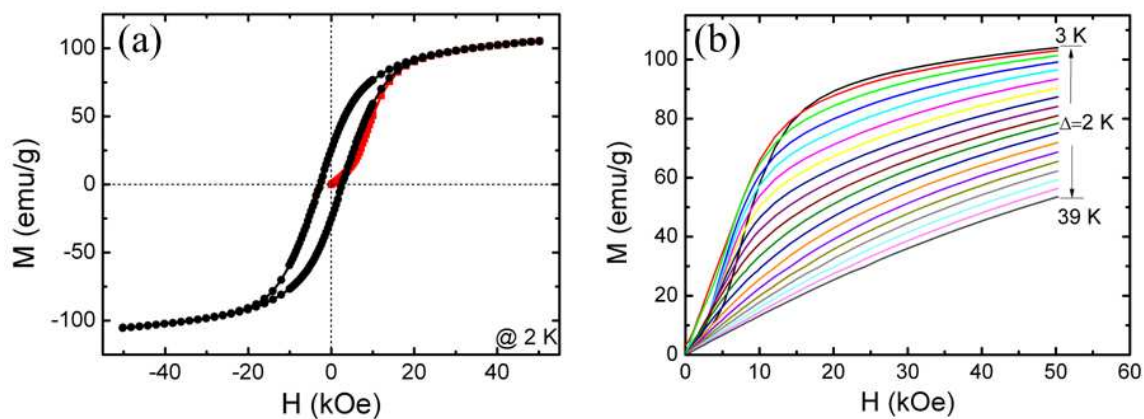
magnetic susceptibility.

FIG.4. (Color online) (a) The magnetic hysteresis loops of Tm_5Ge_4 measured in ZFC conditions. The initial magnetization curves are marked in red color. (b) Isothermal magnetizations versus applied magnetic field where the magnetizations are measured under an increasing magnetic field.
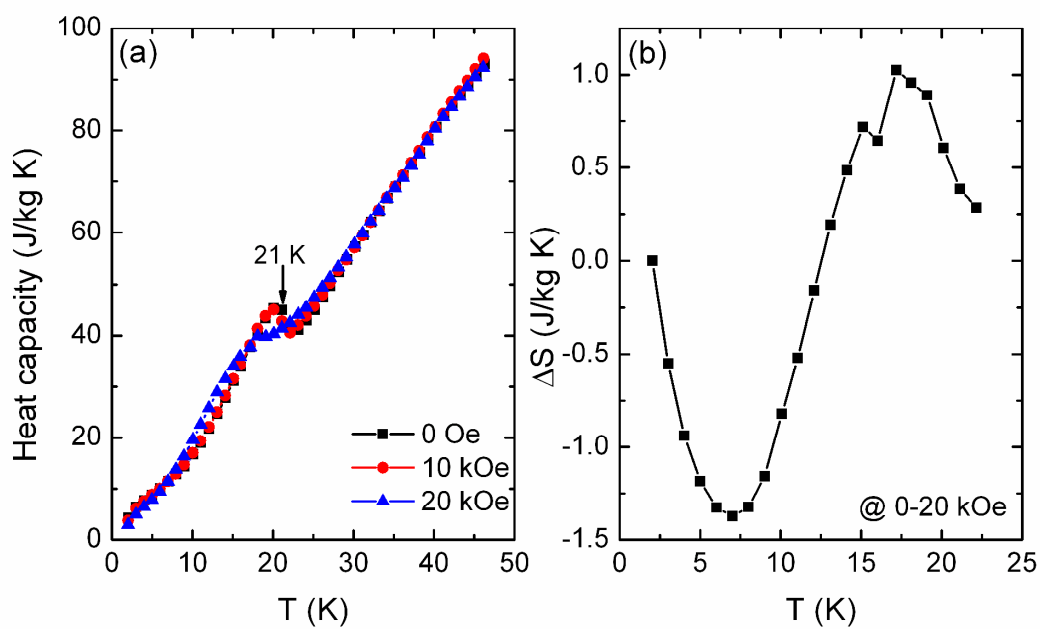
FIG.5. (Color online) (a) The heat capacity of Tm_5Ge_4 measured as a function of temperature and magnetic field. (b) The entropy change calculated by heat capacity data in ΔH=20 kOe magnetic field.